Compact in-plane channel drop filter design using a single cavity with two degenerate modes in 2D photonic crystal slabs

Ziyang Zhang and Min Qiu

Laboratory of Optics, Photonics and Quantum Electronics,
Department of Microelectronics and Information Technology,
Royal Institute of Technology (KTH),
Electrum 229, 164 40 Kista, Sweden,
min@imit.kth.se

Abstract: A compact in-plane channel drop filter design in 2D hexagonal lattice photonic crystal slabs is presented in this paper. The system consists of two photonic crystal waveguides and a single cavity with two degenerate modes. Both modes are able to confine light strongly in the vertical dimension and prove to couple equally into the waveguides. Three dimensional finite difference time domain simulations show that the quality factor is around *3,000*. At resonance, power transferred to the drop waveguide is *78%* and only *1.6%* remains in the bus waveguide. We also show that by carefully tuning the drop waveguide boundary, light remaining in the bus can be further reduced to below *0.4%* and thus the channel isolation is larger than *22dB*.

©2005 Optical Society of America

OCIS codes: (250.5300) Photonic integrated circuits; (230.5750) Resonators; (230.3990) Microstructure devices

References and Links

1. E. Yablonovitch, "Inhibited Spontaneous Emission in Solid-State Physics and Electronics," Phys. Rev. Lett. **58**, 2059 (1987)
2. S. John, "Strong localization of photons in certain disordered dielectric superlattices," Phys. Rev. Lett. **58**, 2486 (1987)
3. H. Benisty, "Modal analysis of optical guides with two-dimensional photonic band-gap boundaries," J. Appl. Phys. **75**, 4753 (1994)
4. A. Mekis, S. Fan, and J. D. Joannopoulos, "Bound states in photonic crystal waveguides and waveguide bends," Phys. Rev. B **58**, 4809 (1998)
5. T. F. Krauss, R. M. De La Rue, and S. Brand, "Two-dimensional photonic-bandgap structures operating at near-infrared wavelengths," Nature **383**, 699 (1996)
6. S. G. Johnson, S. Fan, P. R. Villeneuve, J. D. Joannopoulos, and L. A. Kolodziejski, "Guided modes in photonic crystal slabs," Phys. Rev. B, **60**, 5751 (1999)
7. Y. Akahane, T. Asano, B. S. Song, and S. Noda, "High-Q photonic nanocavity in a two-dimensional photonic crystal," Nature **425**, 944 (2003)
8. H. Y. Ryu, M. Notomi, and Y. H. Lee, "High-quality-factor and small-mode-volume hexapole modes in photonic-crystal-slab nanocavities," Appl. Phys. Lett. **83**, 4294 (2003)
9. Z. Zhang and M. Qiu, "Small-volume waveguide-section high Q microcavities in 2D photonic crystal slabs," Opt. Express **12**, 3988 (2004), http://www.opticsexpress.org/abstract.cfm?URI=OPEX-12-17-3988
10. K. Srinivasan and O. Painter, "Fourier space design of high-Q cavities in standard and compressed hexagonal lattice photonic crystals," Opt. Express **11**, 579 (2003), http://www.opticsexpress.org/abstract.cfm?URI=OPEX-11-6-579
11. M. Tokushima and H. Yamada, "Light propagation in a photonic-crystal-slab line-defect waveguide," IEEE J. of Quantum Electron. **38**, 753 (2002)
12. A. Sugitatsu, T. Asano and S. Noda, "Characterization of line-defect-waveguide lasers in two-dimensional photonic-crystal slabs," Appl. Phys. Lett. **84**, 5395 (2004)
13. M. Qiu and B. Jaskorzynska, "A design of a channel drop filter in a two-dimensional triangular photonic crystal," Appl. Phys. Lett. **83**, 1074 (2003)
14. M. Qiu, "Ultra-compact optical filter in two-dimensional photonic crystal," Electron. Lett. **40**, 539 (2004)

#6586 - $15.00 US Received 11 February 2005; revised 21 March 2005; accepted 22 March 2005
(C) 2005 OSA

15. S. Noda, A. Chutinan and M. Imada, "Trapping and emission of photons by a single defect in a photonic bandgap structure," Nature **407**, 608 (2000)
16. B. S. Song, S. Noda and T. Asano, "Photonic Devices Based on In-Plane Hetero Photonic Crystals," Science **300**, 1537 (2003)
17. A. Chutinan, M. Mochizuki, M. Imada and S. Noda, "Surface-emitting channel drop filters using single defects in two-dimensional photonic crystal slabs," Appl. Phys. Lett. **79**, 2690 (2001)
18. B. K. Min, J. E. Kim and H. Y. Park, "High-efficiency Surface-emitting channel drop filters in two-dimensional photonic crystal slabs," Appl. Phys. Lett. **86**, 11106 (2005)
19. B. K. Min, J. E. Kim and H. Y. Park, "Channel drop filters using resonant tunnelling processes in two-dimensional triangular lattice photonic crystal slabs," Optics Commun. **237**, 59 (2004)
20. K. H. Hwang and G. H. Song, "Design of a Two-Dimensional Photonic-Crystal Channel-Drop Filter Based on the Triangular-Lattice Holes on the Slab Structure," Proceedings of 30th European Conference on Optical Communication, **5**, 76 (Stockholm, Sweden, 2004)
21. S. Fan, Pierre R. Villeneuve, and J. D. Joannopoulos, "Channel Drop Tunneling through Localized States," Phys. Rev. Lett. **80**, 960 (1998)
22. C. Manolatou, M. J. Khan, S. Fan, Pierre R. Villeneuve, H. A. Haus and J. D. Joannopoulos, "Coupling of Modes Analysis of Resonant Channel Add-Drop Filters," IEEE J. of Quantum Electron. **35**, 1322 (1999)
23. Y. Xu, Y. Li, E. K. Lee and A. Yariv, "Scattering-theory analysis of waveguide-resonator coupling," Phys. Rev. E. **62**, 7389 (2000)
24. J. Vučković, M. lončar, H. Mabuchi and A. Scherer, "Optimization of the Q factor in photonic crystal microcavities," IEEE J. of Quantum Electron. **38**, 850 (2002)
25. K. S. Yee, "Numerical solution of initial boundary value problems involving Maxwell's equations in isotropic media," IEEE Trans. Antennas and Propagation, **14**, 302 (1966)
26. J. P. Berenger, "A perfectly matched layer for the absorption of electromagnetic waves," J. Comput. Phys. **114**, 185 (1994)
27. M. Qiu and Z. Zhang, "High Q Microcavities in 2D Photonic Crystal Slabs Studied by FDTD Techniques and Padé Approximation," Proc. SPIE. **5733,** (2005, to be published)
28. W. H. Guo, W. J. Li, and Y. Z. Huang, "Computation of Resonant Frequencies and Quality Factors of Cavities by FDTD Technique and Padé Approximation," IEEE Microwave Wireless Components Lett. **11**, 223 (2001)

1. Introduction

Two-dimensional photonic crystal slabs (2D PCS's), thin dielectric slabs with two-dimensional photonic crystal pattern, have attracted much attention as they provide an in-plane photonic band gap, are able to confine light in the vertical dimension with index guiding and promise easier fabrication than their 3D counterparts [1-6]. Various miniature photonic devices can be realized in 2D PCS's, such as high-Q resonators [7-10], waveguides [11-12] and channel drop filters [13-20], which are the essential components of photonic integrated circuits (PICs) and dense wavelength division multiplexing (DWDM) optical communication systems.

Over the past few years, there have been different designs of channel drop filters in 2D PCS's. One design is the surface-emitting type [15-18], which consists of a waveguide and a cavity system. Input signal from the waveguide tunnels into the cavity and is emitted in the vertical direction. Though in principle all light can be dropped in the vertical direction by using a cavity system with two degenerate modes [18], this design brings up a real challenge when collecting light vertically. Usually light emitted downward cannot be collected due to structural restrictions. The vertical radiation pattern has to be optimized in order to efficiently collect the other *50%* of light emitted upward. The in-plane design involves two waveguides (bus and drop) and a cavity system. Channel to be selected comes from the bus waveguide, tunnels into the cavity and is eventually transferred to the drop waveguide. Theoretical analysis of the in-plane channel drop filter has matured over the years [21-23] and in principle *100%* transfer between two waveguides can be realized if the cavity system provides at least a pair of degenerate modes of opposite symmetry with infinitely high vertical Q factor. Yet very few in-plane designs in 2D PCS's have been reported [19-20]. The bottleneck lies in the cavity system, which largely limits the drop efficiency (loss) and line-width of the filter.

As mentioned earlier, in 2D PCS's light is confined vertically by index-guiding. Though theoretically 2D PCS waveguides can be lossless within a narrow frequency region, cavity

#6586 - $15.00 US Received 11 February 2005; revised 21 March 2005; accepted 22 March 2005
(C) 2005 OSA

modes are always leaky in the vertical direction. For a symmetric in-plane channel drop filter system where the degenerate modes have equal frequency and equal decay rates into both waveguides, the power transmission $|\boldsymbol{T}|^2$ and power dropped $|\boldsymbol{D}|^2$ at resonance can be expressed by [22],

$$|T|^2 = \left(\frac{1}{1+2\tau_o/\tau_e}\right)^2 = \left(\frac{1}{1+2Q_o/Q_e}\right)^2 \approx \left(\frac{1}{1+Q_\perp/Q_\parallel}\right)^2, \quad (1)$$

$$|D|^2 = \left(\frac{2}{2+\tau_e/\tau_o}\right)^2 = \left(\frac{2}{2+Q_e/Q_o}\right)^2 \approx \left(\frac{1}{1+Q_\parallel/Q_\perp}\right)^2, \quad (2)$$

where $1/\tau_o$ is the decay rate due to loss and $1/\tau_e$ is the decay rate into either waveguide. The decay rate is related to Q factor by $Q_o = \omega_0\tau_o/2$ and $Q_e = \omega_0\tau_e/2$. If the resonant frequency ω_0 of the cavity modes lies within the lossless region of the waveguide, the total loss of the system is mainly from the vertical loss of the cavity, i.e., $Q_o \approx Q_\perp$, where $Q_\perp$ is the vertical Q factor of the cavity. The in-plane Q factor ($Q_\triangleleft$) of the cavity is related to Q_e by $Q_\triangleleft = Q_e/2$ if we assume the cavity modes decay into both waveguides equally and ignore the in-plane loss due to the limited number of lattice surrounding the system. From equation (1) and (2), we can see the direct relation between the drop efficiency and the ratio $Q_\perp/Q_\triangleleft$. For example, in order to have $|\boldsymbol{D}|^2 > 80\%$, $Q_\perp$ should at least be 10 times larger than $Q_\triangleleft$. The choice of high Q cavity is critical and has not yet been well addressed in the previous designs. In Ref. [19] $Q_\perp$ is only a few times larger than $Q_\triangleleft$, the power transferred to the drop waveguide is only *61%* and *5%* still remains in the bus. In Ref. [20], the resonant frequency of the cavity mode lies beyond the lossless region of the waveguide, which further increases vertical loss. In both designs the degenerate modes are provided by two identical single-mode cavities separated by a distance, which not only makes the device larger and more loss-prone, but also raises difficulties for fabrication, since it is not yet likely to produce two identical cavities or to determine their positions precisely using present etching techniques.

In this paper, we come up with a compact design of in-plane channel drop filter in 2D PCS's with a single cavity that supports two high Q modes. We will show the process of tuning the two modes, even and odd, into exact frequency degeneracy with similar Q⊥ and Q◁ values. When the transmission spectra are achieved, we will discuss how to improve the channel isolation efficiently. For computations of cavity modes and simulations of wave propagation, we use our home-made 3D finite difference time domain (3D FDTD) code with perfect matched layer boundary conditions [25-26]. When we analyze the individual cavity modes, we apply mirror boundary conditions in the x, y, and z directions, which reduces the computation size to one-eighths and also allows us to study the even and odd modes separately [9]. A combination of FDTD techniques and Padé approximation with Baker's algorithm [27-28] is used for the cavity mode Q factor calculations. The total computation domain is 18a×19.06a×4a along the x, y and z directions, where a is the lattice constant. The grid size is 0.05a in the x, z direction and 0.0433a in the y direction.

2. Cavity design and modes tuning

Though there have been designs of cavities in 2D PCS's with $Q_\perp$ larger than 10^6 [8-9], we find them deteriorate tremendously when used in the in-plane channel drop filter system. The reason lies in the presence of the waveguides. Most high Q cavities reported involve some missing air holes and their high $Q_\perp$ is achieved by carefully modifying the surrounding boundaries so that in the momentum (***k***) space, most of the components are pushed away from the light cone [7-9, 24]. However, when the waveguides are placed close to the cavity, the boundaries of the cavity are changed and so is the ***k*** space distribution of the cavity mode. As a result, more ***k*** components are introduced into the light cone and thus $Q_\perp$ is reduced greatly.

#6586 - $15.00 US Received 11 February 2005; revised 21 March 2005; accepted 22 March 2005
(C) 2005 OSA

Though increasing the distance between the waveguide and the cavity can reduce the waveguide's impact on $Q_{\perp}$ of the cavity, this will reduce the coupling between the waveguide and the cavity, $Q_{\triangleleft}$ is also increased and the ratio $Q_{\perp}/Q_{\triangleleft}$ may not improve at all.

To avoid the dilemma mentioned above, we seek to use a cavity whose vertical light confinement does not rely much on the surrounding boundaries [10]. The structure of the cavity is shown in Fig. 1(a). This cavity is constructed by a central large air hole with radius R_0, surrounded by 4 periods of air holes with decreasing radii, along the outward direction denoted by R_1, R_2, R_3, and R_4 respectively. The radius of the air holes on the same hexagon stays the same and R_1 to R_4 follows a parabolic pattern as shown in equation (3). The radius of air holes on the outmost hexagon R_4 is the same as the regular air hole radius $R = 0.30a$, where a is the lattice constant and set to $420nm$ in our case. The slab thickness t is $0.6a$ and the refractive index n of the slab is 3.4, corresponding to silicon at $1.55\mu m$. If R_0 and R_1 are given, the cavity structure is determined.

$$R_m = R_1 - (m-1)^2 (R_1 - R_4)/9; m = 1,2,3,4. \tag{3}$$

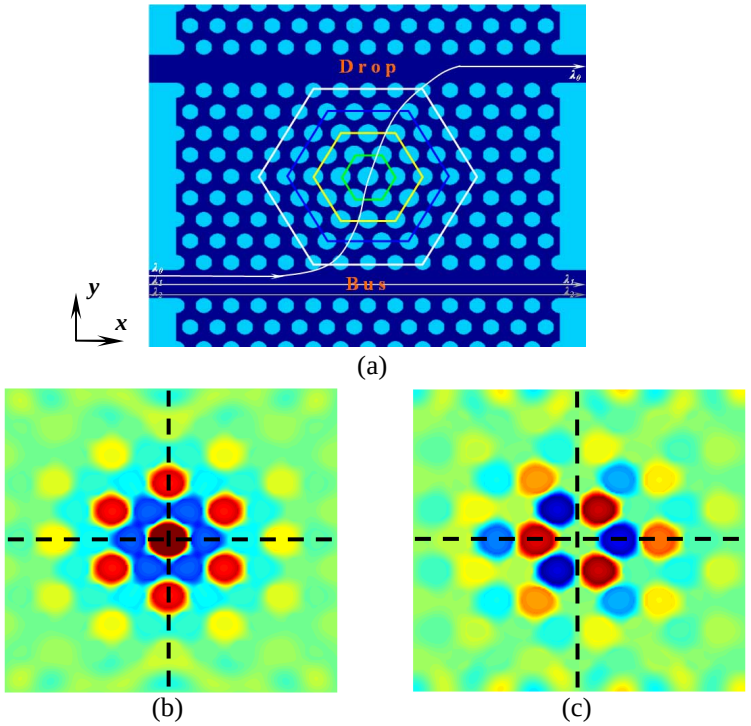

Fig. 1. (a) Top view of the system. Selected channel is transferred along the forward direction of the drop waveguide. The cavity involves a central large air hole surrounded by 4 hexagons of lattice. The radii of air holes on the hexagons are tuned into a graded pattern following equation (3). (b) H_z field distribution of the even mode at central slab plane. (c) H_z field distribution of the odd mode at central slab plane. The mirror planes are shown as the dashed lines.

This cavity consists of two-levels of vertical light confinement [10]. The first level of confinement has a centrally enlarged air hole (R_0) followed by a relatively large decrease in hole radius (R_1) for the nearest neighbor holes. The hole radii are then parabolically decreased in moving radially outwards down to $R_4 = R$ at the edge of the cavity, forming the second level of confinement. Though increasing the number of hexagons surrounding the central large hole can enhance the vertical light confinement, it also reduces waveguide-cavity coupling. We choose the number of surrounding hexagons to be 4, which is sufficient to keep good waveguide-cavity coupling while maintaining high vertical Q. The hexagonal symmetry

#6586 - $15.00 US Received 11 February 2005; revised 21 March 2005; accepted 22 March 2005
(C) 2005 OSA

of the cavity itself makes it possible to support two modes of opposite symmetries (though only the mode with H_z field even in both in-plane directions was reported in [10]). As shown in Fig. 1(b) and 1(c), the first mode has H_z field even in both x and y directions and the second mode has H_z field even along y direction but odd along x direction. Their symmetry properties decide a forward drop when the two modes are degenerate [22].

The cavity structure has to be fine-tuned in order to force the even and odd mode into degeneracy, i.e., the two modes should have the same resonant frequency and similar, if not exactly the same, Q factors. We can see from Fig. 1(b) and 1(c) that the even mode has strong field distribution on the central air hole region, while the odd mode tends to concentrate on the first-round neighboring holes, so we expect that modification of R_0 parameter will have more impact on the even mode and so it is with R_1 on the odd mode. In order to maintain the vertical light confinement of the cavity, we keep $R_0 > R_1$ and follow Eq. (3) strictly during the tuning process. We start with $R_0 = 0.365a$ and increase R_0 by step of $0.005a$ to $0.395a$. For each value of R_0, we choose three values for R_1, i.e., $R_1 = R_0 - 0.005a$, $R_1 = R_0 - 0.01a$ and $R_1 = R_0 - 0.015a$. The results are shown in Fig. 2.

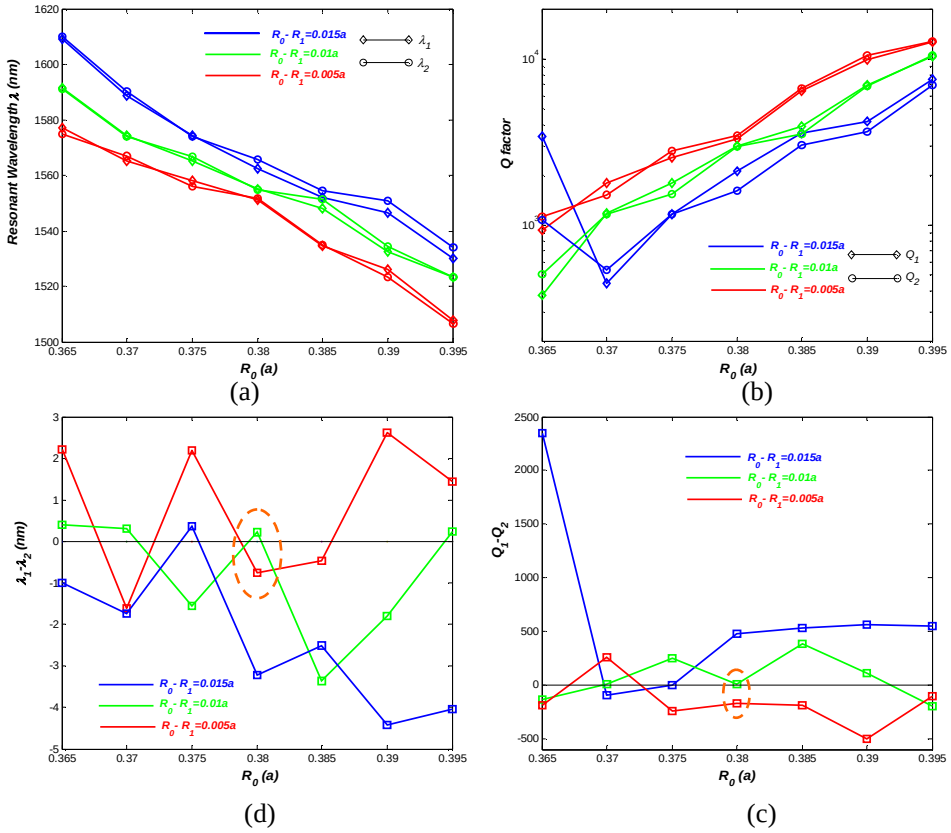

Fig. 2. Tuning of the cavity shown in Fig. 1(a). The lattice constant a is $420nm$. (a) Variations of central wavelengths of the two modes. (b) Variations of total Q factors. (c) Central wavelength difference shifts. (d) Q factor difference shifts. The region inside the dashed circle is the work region, where the two modes have closest central wavelengths and Q factors.

Figure 2(a) shows the central wavelengths of the two modes with respect to R_0 and R_1. The central wavelength of the even mode λ_1 is labeled with diamond maker and λ_2 of the odd mode is labeled with circle maker. The Q factor variations of the two modes are shown in Fig. 2(b). Q_1 is the total Q factor of the even mode and Q_2 is the total Q factor of the odd mode. Fig. 2(c) and 2(d) show the central wavelength and Q factor difference respectively. Examine Fig. 2(c) and 2(d) in detail and we find the two modes have the closest central wavelengths

#6586 - $15.00 US Received 11 February 2005; revised 21 March 2005; accepted 22 March 2005
(C) 2005 OSA

and Q factors when $R_0 = 0.38a$ and $R_0 - 0.005a > R_1 > R_0 - 0.1a$. We set $R_0 = 0.38a$ and tune R_1 in smaller steps. The result shows when R_1 is $0.372a$, the two modes have closest central wavelengths as well as Q factors, with $\lambda_1 = 1554.51nm$, $\lambda_2 = 1554.52nm$, $Q_1 = 3{,}060$ and $Q_2 = 3{,}020$. Further computation separates $Q_\perp$ and $Q_\lhd$ from Q total by $Q^{-1} = Q_\perp^{-1} + Q_\lhd^{-1}$. For the even mode, $Q_{\perp 1} = 40{,}500$ and $Q_{\lhd 1} = 3{,}100$. For the odd mode, $Q_{\perp 2} = 35{,}000$ and $Q_{\lhd 2} = 3{,}050$. The central wavelength difference is smaller than $0.01nm$ and is negligible compared to the line width.

We have already seen from Fig. 2 that the even and odd modes have a strong tendency to degenerate. For a few tests, we vary the refractive index n of the silicon slab by $\pm 1\%$ and also the slab thickness t by $\pm 0.05a$, the two modes stay degenerate with $\Delta\lambda < 0.01nm$ and $\Delta Q < 100$, despite the absolute shift in central wavelength and Q factors. This makes our design insensitive to some of the fabrication uncertainties, such as slab thickness and material index.

Furthermore, the waveguide mode is single, non-leaky and not highly dispersive in the frequency range $0.267 \sim 0.28\ (c/a)$, corresponding to $1500 \sim 1573\ (nm)$ in wavelength assuming lattice constant $a = 420\ nm$. The waveguide loss is avoided in our system as the central wavelengths of the cavity modes lie within this range.

The 3D FDTD simulation result for the transmission computation is shown in Fig. 3. At resonance, 78% of light is transferred along the forward direction of the drop waveguide, 1.75% is transferred along the backward direction of the drop waveguide, and 1.6% of light is still left in the bus waveguide. The Q factor measured as full width half maximum (FWHM) of the transmission spectrum is around $3{,}000$, relevant to the previous $Q_\lhd$ calculations.

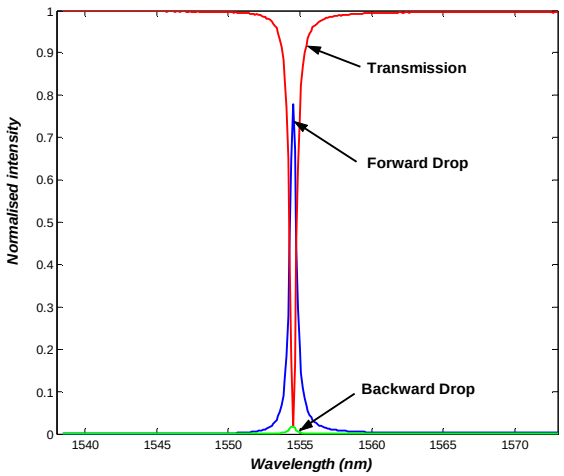

Fig. 3. Intensity spectra for the structure shown in Fig. 1(a). The wavelengths correspond to a lattice constant of $420nm$.

3. Waveguide tuning to improve the drop effect

One important factor characterizing a channel drop filter is its channel isolation (*CI*), defined as $CI = 10\log(P_1/P_2)$, where P_1 and P_2 are the power of the selected channel transferred to the drop waveguide and the power remaining in the bus respectively. The channel isolation should be as large as possible to avoid the cross talk. The *CI* value of the system we designed above is only $16.9\ dB$. We try to improve it by further reducing the 1.6% of light that remains in the bus while keeping the power transferred high. We re-write Eq. (1) in more detail. In equation (4) below, $1/\tau_{e1}$ and $1/\tau'_{e1}$ are the decay rate of the even mode into bus and drop

#6586 - $15.00 US Received 11 February 2005; revised 21 March 2005; accepted 22 March 2005
(C) 2005 OSA

waveguide respectively, $1/\tau_{o1}$ is the decay rate of the even mode due to loss and similarly defined are $1/\tau_{e2}$, $1/\tau'_{e2}$ and $1/\tau_{o2}$ for the odd mode.

When the system is symmetric and each mode decay equally into bus and drop waveguide, we have $1/\tau_{e1} = 1/\tau'_{e1}$ and $1/\tau_{e2} = 1/\tau'_{e2}$. In this case, $|\boldsymbol{T}|^2$ will always be larger than zero according to equation (4) and the selected channel cannot be *100%* dropped. However, if we modify the waveguide boundary and let $\tau'_{e1,\ 2}$ slightly larger than $\tau_{e1,\ 2}$ so that the nominator of Eq. (4) becomes zero, the input signal power at resonant wavelength is completely removed from the bus.

$$|T|^2 = \left(1 - \frac{\frac{1}{\tau_{e1}}}{\frac{1}{\tau_{e1}} + \frac{1}{\tau'_{e1}} + \frac{1}{\tau_{o1}}} - \frac{\frac{1}{\tau_{e2}}}{\frac{1}{\tau_{e2}} + \frac{1}{\tau'_{e2}} + \frac{1}{\tau_{o2}}}\right)^2$$

$$= \left(\frac{\frac{\tau_{e1}}{\tau'_{e1}} \cdot \frac{\tau_{e2}}{\tau'_{e2}} + \frac{\tau_{e1}}{\tau'_{e1}} \cdot \frac{\tau_{e2}}{\tau_{o2}} + \frac{\tau_{e1}}{\tau_{o1}} \cdot \frac{\tau_{e2}}{\tau'_{e2}} + \frac{\tau_{e1}}{\tau_{o1}} \cdot \frac{\tau_{e2}}{\tau_{o2}} - 1}{\left(1 + \frac{\tau_{e1}}{\tau'_{e1}} + \frac{\tau_{e1}}{\tau_{o1}}\right)\left(1 + \frac{\tau_{e2}}{\tau'_{e2}} + \frac{\tau_{e2}}{\tau_{o2}}\right)}\right)^2, \qquad (4)$$

As shown in Fig. 4, we reduce the radius R_w of the air holes at the upper boundary of the drop waveguide. This modification turns out to affect both modes equally. The in-plane Q factors of both modes are improved and thus $\tau'_{e1,\ 2}$ increased to the same extent. The two modes stay degenerate though their central wavelengths shift slightly by the same amount. There are other ways to change the decay rates, such as enlarging the air hole radius of the bus waveguide boundaries and increasing the drop waveguide width. These changes, however, are too abrupt and difficult to control, so we have skipped them in this paper.

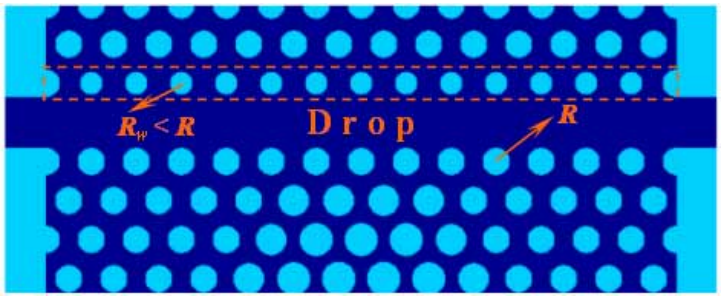

Fig. 4. The radius of air holes on the upper boundary of the drop waveguide is modified into R_w in order to reduce the signal power remained in the bus waveguide.

The simulation result is shown in Table 1 below. At $R_w = 0.27a$, only *0.39%* of signal power remains in the bus waveguide and the channel isolation is enhanced to *22.7dB*. It is worth noting that due to the Lorentian line shape of the transmission spectra [22], the filter undergoes fairly large interchannel cross talk. The Q factor of the filter is around *3,000* and if we use *100GHz* channel spacing centered at the resonant frequency, the interchannel cross talk level is only *13dB* below the desired channel. A higher Q factor is desired in the future channel drop filter designs using 2D PCS's.

#6586 - $15.00 US Received 11 February 2005; revised 21 March 2005; accepted 22 March 2005
(C) 2005 OSA

Table 1. Signal power remained and transferred at resonance with different R_w

R_w (a)	Signal power remained in bus	Signal power transferred to drop	Channel Isolation (CI)	Central Wavelength (nm)
0.30	**1.63%**	**77.9%**	**16.79**	**1554.52**
0.28	**0.91%**	**76.6%**	**19.23**	**1554.55**
0.27	**0.39%**	**73.8%**	**22.73**	**1554.63**
0.26	**0.99%**	**66.2%**	**18.23**	**1554.66**

Figure 5 shows the oscillation of the steady-state field distribution (H_z) at the resonant frequency for the case $R_w = 0.27a$. A silicon wire is connected to each end of the photonic crystal waveguides. Most of the field is transferred along the forward direction of the drop waveguide. The field along the forward direction of the bus waveguide and along the backward direction of the drop waveguide is negligible. Also note that the field is much stronger in the cavity region due to the high Q factor (~*3,000*). The filter is compact and only occupies an area of a few wavelengths square.

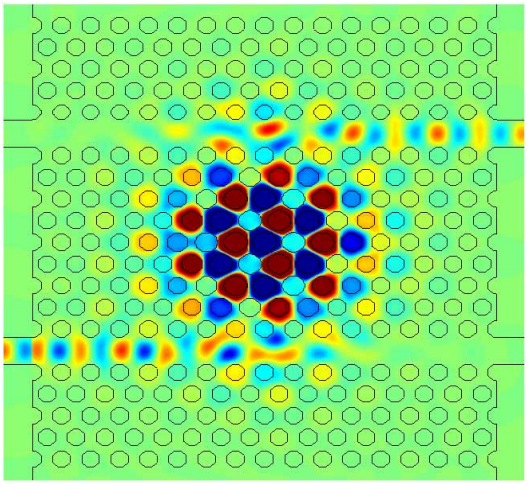

Fig. 5. Steady state H_z field oscillation at resonant frequency for the structure shown in Fig. 1(a) and 4, with R_w=*0.27*. (Movie 1,293 KB)

4. Conclusions

To conclude, we have successfully designed an in-plane channel drop filter in 2D hexagonal lattice photonic crystal slab. The system is compact and only involves a single cavity, which is constructed by arranging the radii of air holes on a few hexagons into a graded pattern. The cavity supports two modes of opposite symmetry. Both modes keep high vertical Q and the system undergoes low vertical loss. By carefully tuning the cavity, the two modes can achieve degeneracy. For a lattice constant of 420nm, the selecting wavelength is 1554.52nm and the line width of the filter is around 0.52nm corresponding to a Q factor of 3,000. At resonance, the signal power transferred along the forward direction of the drop waveguide is 78% and 1.6% remains in the bus. By modifying the upper boundary of the drop waveguide, light remaining in the bus can be further reduced to below 0.4%, with channel isolation enhanced to 22.7 dB. We believe this novel and compact design is adequate for dense wavelength division multiplexing applications in modern optical networks.

#6586 - $15.00 US Received 11 February 2005; revised 21 March 2005; accepted 22 March 2005
(C) 2005 OSA

Acknowledgments

This work was supported by the Swedish Foundation for Strategic Research (SSF) on INGVAR program, the SSF Strategic Research Center in Photonics, and the Swedish Research Council (VR) under project 2003-5501.

#6586 - $15.00 US Received 11 February 2005; revised 21 March 2005; accepted 22 March 2005
(C) 2005 OSA